Available online at www.sciencedirect.com
SCIENCE DIRECT®
Journal of Power Sources 118 (2003) 129–149
JOURNAL OF POWER SOURCES
www.elsevier.com/locate/jpowsour

Modelling results for the thermal management sub-system of a combined heat and power (CHP) fuel cell system (FCS)

Whitney G. Colella*

Department of Mechanical Engineering, Stanford University, Stanford, CA 94305, USA

Abstract

Although the fuel cells research and development community has traditionally focused the majority of its efforts on improving the fuel cell stack's voltage (electrical efficiency), combined heat and power (CHP) fuel cell system (FCSs) may achieve a competitive advantage over conventional generators only if the research and development community refocuses its efforts on cultivating other inherent technical qualities of such systems. Based on an analysis of their use within energy markets, these inherent qualities include (1) an ability to vary their electrical load rapidly, (2) an ability to vary their heat to power ratio during operation, and (3) an ability to deliver their waste heat to a useful thermal sink. This article focuses on the last of three design objectives: effectively capturing heat from a CHP FCS. This article (1) delineates the design specifications for a 6 kWe CHP FCS, (2) analyses four possible cooling loop configurations for this system, and (3) concludes which one of these provides the optimal heat recovery performance.
© 2003 Published by Elsevier Science B.V.

Keywords: Fuel cell system (FCS); Combined heat and power (CHP); Domestic heating (cooling) loop; Thermal and electrical efficiency; English electricity market structure; Pinch Point Analysis

1. Introduction: energy markets and thermal loop analysis

For fuel cell systems (FCS) to achieve a genuine financial and environmental advantage over competing technologies, they must not only produce electricity at a high efficiency, but also useful heat. A combined heat and power (CHP) fuel cell system (FCS) provides both useful electricity and heat directly onsite to a building. In practice, most CHP FCSs first use a fuel reforming process to convert a readily-available hydrocarbon fuel such as natural gas into a hydrogen rich gas, which is then consumed within a fuel cell to produce electricity and heat. Due to the importance of recovering heat in the design of a CHP FCS, this article analyses different configurations for a CHP FCS heating loop [1].

Although a CHP FCS may deliver all of its electricity and heat to a single building, it may also supply them to a network of buildings by acting as an embedded generator. An embedded generator is a decentralised generator in close proximity to consumers that feeds part of its electricity into a local low-voltage electricity distribution network, part of its heat into a local community heating network, and, in some cases, part of the remaining electricity and heat to a direct source of demand onsite [2]. Such a CHP FCS acting as both an embedded electricity and thermal generator is shown in Fig. 1, the first fuel cell system commercially-installed in Great Britain, providing heating, cooling, and electricity to the town of Woking's Leisure Centre [3]. Because of the importance of these systems in providing not only electricity but also useful heat [4], this article discusses a similar CHP FCS with a strong focus on the design of that unit's heating loop.

1.1. Implications of the structure of energy markets for the design of combined heat and power fuel cell systems

The importance of recovering heat from a CHP FCS is two-fold: a network of CHP FCSs may be able to achieve both (1) a more efficient operating point for an economy, and (2) a more environmentally benign [5] operating point for a community. These benefits can arise from the way in which these units might operate as a network within their surrounding electricity and heating markets, in contrast to conventional power generators.

Conventional power generation suffers from dual economic and environmental inefficiencies. These arise because (a) electricity markets exhibit a high volatility in electricity demand, and (b) most conventional electric power generators

* Tel.: +1-650-283-2701; fax: +1-530-869-7676.
E-mail address: wcolella@alumni.princeton.edu (W.G. Colella).

0378-7753/03/$ – see front matter © 2003 Published by Elsevier Science B.V.
doi:10.1016/S0378-7753(03)00071-5

Fig. 1. Mr. Allan Jones, the Energy Services Manager of the Woking Borough Council, spearheaded the implementation of Britain's first commercial combined heat and power fuel cell system. The 250 kWe ONSI unit, produced by International Fuel Cells Inc., began in 2002 to provide heating, cooling, and electricity to Woking Park's swimming pool and leisure complex. Shown with Colella.

dispose of their heat to the environment rather than applying it to a useful purpose. These economic and environmental inefficiencies, and these two causes behind them, are summarised in the matrix shown in Table 1. With respect to the top left-hand corner of the matrix that refers to (1) the economic inefficiencies resulting from (a) a high volatility in electricity demand, an economy suffers from a dead-weight social loss (a financial loss to the economy) because ''instantaneous power'', under volatile conditions, can only be provided by a few generators, thereby leading to oligopolistic (non-competitive) pricing in the market segment for ''instantaneous power''. Electricity markets exhibit large instantaneous surges in the demand for electricity, which cause the instantaneous price of electricity to fluctuate dramatically. Large variations in electricity price result from rapidly varying levels of electricity demand combined with a limited number of electricity suppliers who can respond rapidly to these changes in demand (for example see [6]). Under these conditions, the supply of electricity is restricted. A lack of competition among a smaller number of generators who can supply ''instantaneous power'' leads to a higher price for electricity than in a competitive market, and the extent of the difference between the competitive electricity price and the non-competitive one is proportional to the financial loss to the economy. Also with respect to (a) a high volatility in electricity demand, as shown by the top right-hand corner of Table 1 matrix, the environment suffers. First, under conditions of volatile electricity demand, the environment suffers from the pollution due to the overproduction and consequent dumping of electricity that the market instantaneously decides it does not need. Second, the environment suffers from the marginally greater pollution incurred by meeting peaks in electricity demand, which often involves switching on the most polluting generating plants (typically old oil plants). Table 1 summarises the dual economic and environmental efficiencies that arise from (a) a high volatility in demand in electricity markets. Table 1 also summaries the dual economic and environmental efficiencies that result from (b) conventional power generators dumping most of their by-product heat to the environment, as shown by the bottom row of the matrix. With respect to (b) this disposal of heat, the economy suffers from a dead-weight social loss because customers want to buy the waste heat from power generators but cannot. Anytime a product is created, and customers would like to purchase that product, but cannot, the economy incurs an economic loss. Also with respect to (b) the disposal of heat by generators, the environment suffers. First, the environment suffers from the pollution created during the production of the heat by an electrical power generator that is not usefully consumed. Second, the environment suffers a second time from the pollution created by the boilers or furnaces that do provide for the heat that is demanded, which could have been avoided had the electrical power generator's waste heat been used instead. These points, summarised in Table 1, are explained in greater detail in Section 1.

Both of these (1) economic inefficiencies, and (2) environmental inefficiencies may be attenuated by operating a distributed network of CHP FCS with a particular design focus. One scenario for correcting for this dual economic

Table 1
Electricity markets based on conventional electrical power generation suffer from economic and environmental inefficiencies

	Economic inefficiency	Environmental inefficiency
Electricity markets exhibit a high volatility in demand	The economy suffers from a dead-weight social loss because ''instantaneous power'' can only be provided by a few generators, thereby leading to oligopolistic (non-competitive) pricing in the market segment for ''instantaneous power''	The environment suffers twice from high electricity demand volatility: (1) from the pollution due to the overproduction and consequent dumping of electricity, and (2) from the marginally greater pollution incurred by switching on the most pollutive generating plants (typically old oil plants) to meet demand peaks
Conventional power generators produce heat that is not usefully consumed	The economy suffers from a dead-weight social loss because customers want to buy the waste heat from power generators but cannot	The environment suffers twice from wasted heat: (1) from the pollution created during the production of the wasted heat, and (2) from the pollution created during the production of the additional heat that must be newly created to suffice heat demand

and environmental inefficiency in the power generation market is to operate a network of distributed power plants (such as CHP FCSs) with (i) a greater ability to respond to instantaneous changes in electricity demand, and (ii) a greater ability to expel heat towards a useful purpose. CHP FCSs are a particular technology that enables these two gains. First of all, CHP FCSs, like batteries (but unlike engines, electrical generators, and large-scale power plants), can respond rapidly to changes in electric load. Second of all, CHP FCSs can be designed to more closely match changes in thermal and electrical demands by quickly and efficiently switching between thermal and electrical production by altering their heat to power ratio during operation [7]. Finally, like other distributed generators (but unlike the majority of traditional centralised power stations in practice), CHP FCSs, if installed at the location of a thermal load or network, can be designed to usefully expel waste heat to a local thermal sink. This article discusses in greater detail in the Experimental and Results sections the third aspect of this scenario: design strategies for a CHP FCSs so that they can usefully capture heat onsite for a building.

1.1.1. Conventional generation suffers from dual economic and environmental inefficiencies because of high volatility in electricity demand

1.1.1.1. Economic inefficiencies due to high volatility in electricity demand

1.1.1.1.1. Electricity price varies rapidly and extensively with time. Electricity markets exhibit large instantaneous surges in demand, combined with short-term lags in supply, which cause the real-time price of electricity to fluctuate dramatically over the same short time period. The price of electricity over the course of a single day varies significantly with time, as shown in Fig. 2. Fig. 2 shows the variation in the England's electricity price over half-hourly segments during the course of 1 day [8]. On this particular day, the electricity price varies by a factor of over 1000. The electricity price varies even more significantly over the course of an entire year, as shown in Fig. 3. Fig. 3 shows a histogram of the electricity price in England at every half-hour during 1 year (1998). Fig. 3 shows a power lognormal distribution in electricity price, with a mode between 1.5 and 2.0 pence/kWh, and a large electricity price range, between 0.002 pence/kWh and 27.297 pence/kWh, a price differential of more than 20,000. Such large variations in price are characteristic of all electricity markets throughout a single day and through every day in a year. (However, because electricity markets have different economic structures, not all can show these price fluctuations explicitly, as the data for England's market does.)

1.1.1.1.2. Aggregate electricity demand varies rapidly and extensively with time. Large variations in electricity price result from (1) rapidly varying levels of electricity demand combined with (2) more slowing responding electricity supply. Electricity demand varies rapidly and extensively with time, as shown in Figs. 2 and 4. Fig. 2 shows that the daily variations in price result in part from changes in demand. Fig. 2 shows, over the same period of price fluctuation, an estimate of the total English electricity demand during that period, the total grid system demand (TGSD), projected by the UK's National Grid 1 day in advance. Please note that the TGSD gives a useful general estimate for the total electricity demand for the region during that period, but that the actual demand is much more volatile (like the price). Fig. 2 is still useful for showing the degree to which electricity demand impacts electricity price. For example, as the demand for electricity increases through the morning from 6 a.m. to 9 a.m., given a limited supply, so does the price. Fig. 4 gives a more accurate indication of the degree to which electricity demand can vary with time on the

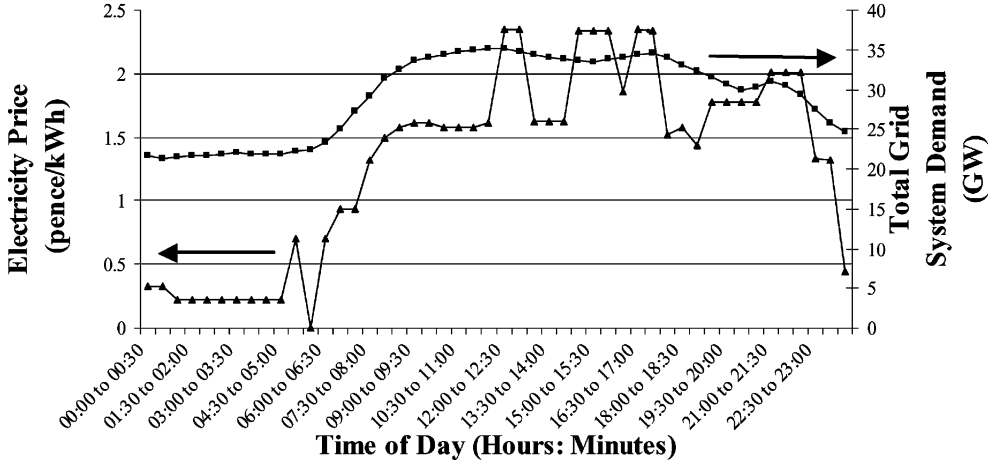

Fig. 2. Illustration of a wide variation in electricity price over time. The electricity price shown here, known as the pool purchase price, was determined via a competitive bidding process among most electricity generators in England for every half-hour segment during a day (3 August 1998).

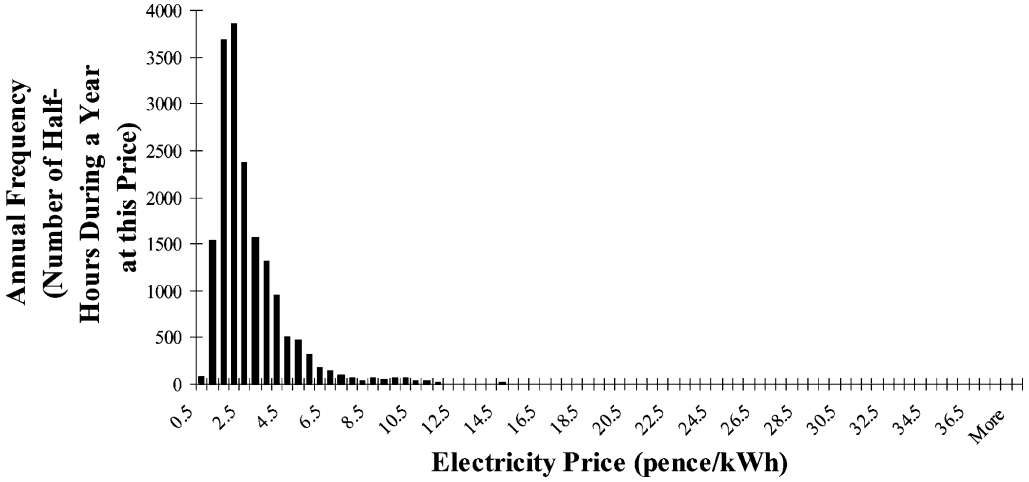

Fig. 3. Electricity price varies over a wide range over 1 year, between 0.002 pence/kWh and 27.793 pence/kWh, a factor of over 20,000. This large range in price indicates deficiencies in being able to match instantaneous electricity demand with that supplied.

aggregate (regional) level [9]. It shows that the cumulative variation in electricity demand for several different English households in the same region over the course of a single day; demand is volatile. In response to this volatile electricity demand, the instantaneous price for electricity is also volatile.

1.1.1.1.3. Electricity demand varies rapidly because consumers are insensitive to changes in the instantaneous price of electricity. Electricity demand varies rapidly because consumers are not sensitive to changes in the instantaneous price of electricity. Aggregate electricity demand varies rapidly primarily in response to changes in consumer tastes, which, are themselves entirely insensitive to changes in electricity price. Consumer tastes include, for example, the way individuals use electrical appliances, lighting, and electronic devices. Other influences, such as the change in weather conditions and the timing of daylight hours, also have a significant impact on aggregate electricity demand but over a longer time horizon. In most electricity systems, consumer tastes in the use of electricity are not impacted by the electricity price in the short-term time horizon. Fig. 5 shows that the aggregate (regional) demand curve for electricity throughout England is nearly perfectly price inelastic, i.e. insensitive to changes in electricity price. Price elasticity of demand (supply) is defined as

$$\text{elasticity of demand (supply)} = \frac{\text{percentage change in quantity demanded (supplied)}}{\text{percentage change in price}}$$

Therefore, a perfectly inelastic demand curve is completely vertical. Instantaneous electricity demand does not vary in response to changes in instantaneous electricity price; on the aggregate and individual levels, the demand for electricity is nearly perfectly price inelastic (for example see [10]). Instantaneous electricity demand is nearly perfectly price inelastic because information about the real-time electricity price is almost never conveyed to consumers. In most electricity systems, consumers are charged a fixed price for electricity, regardless of its underlying real-time price. In this way, the price inelasticity of electricity demand

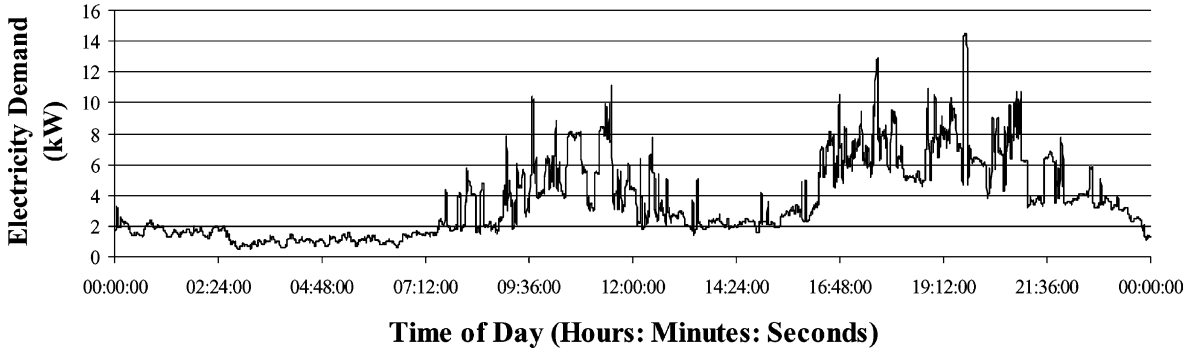

Fig. 4. The cumulative electricity demand of five English homes over 1 day (20 January 2001). The cumulative electricity demand shows a high degree of volatility, and, in this way, is representative also of the high degree of volatility in the aggregate electricity demand across a region.

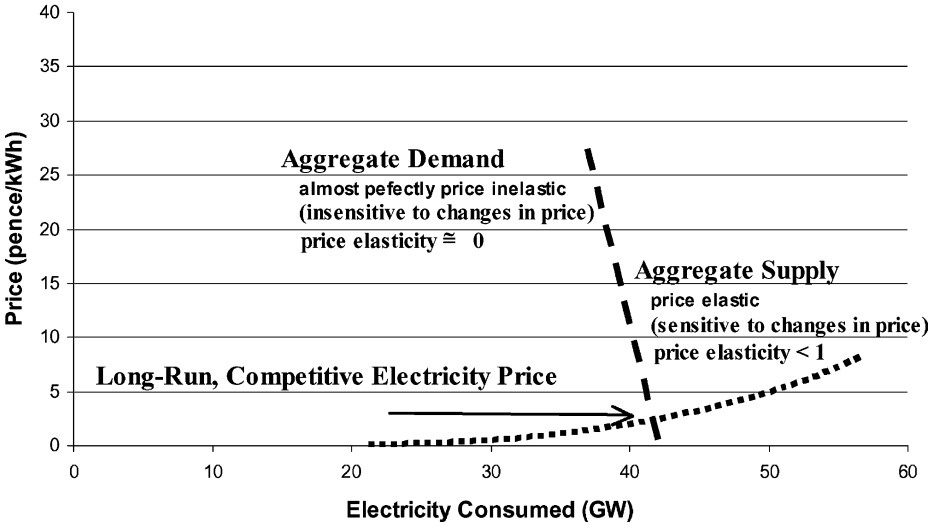

Fig. 5. The aggregate supply and demand for electricity in England. Demand is characteristically inelastic (insensitive to changes in price). In the long-run, electricity markets achieve a stable equilibrium between supply and demand at a relatively low, competitive price.

contributes significantly to the volatility of both electricity demand and consequently electricity price.

1.1.1.1.4. Electricity price varies because instantaneous demand outpaces supply. Having shown the strong impact that rapidly varying levels of electricity demand has in creating large variations in electricity price, the other simultaneous contributing factor to these large variations in electricity price is the lag-time in the supply of electricity. The primary reason that supply lags demand is that the number of electricity generators that can supply instantaneous electricity (or quickly remove their supply) is much smaller than the overall market of electricity generators. Only certain types of generators have this technical quality, which gives them a competitive business advantage in the segment of the electricity market dealing with rapid, unplanned changes in demand.

Electricity supply varies less rapidly than demand for several reasons. First of all, supply lags demand because of delay times in mechanically turning down and ramping up the power output levels of power generators. For example, combined cycle gas turbine plants may take several minutes to alter their power levels while nuclear power plants may take several hours. For this reason, the number of electricity generators that are able to rapidly vary their output is much smaller than that for the overall market; the market concentration of generators in this segment of the market is much greater. Second of all, supply lags demand because unlike most commodities, electricity cannot at present be economically stored for future use. As a result of this particular quality of electricity, and also as a result of legislation commonly requiring supply of electricity as a resource equally to individuals, the instantaneous supply must meet instantaneous demand. Third of all, supply lags demand, in some cases, because of collusive efforts among electricity generators and/or fuel suppliers to purposely restrict supply of a resource to increase its price. Because only a small number of electricity generators are able to supply electricity to a market in a rapidly variable manner, in this segment of the electricity market, dealing with rapid downturns and upturns in supply, the concentration of companies is lower, making it easier to collude. In this market segment, in the past, electricity generators or fuel suppliers have colluded amongst themselves to either directly raise the price they bid for supplying electricity or fuel, or to indirectly do so by agreeing to limit their supply over fixed time periods. For example, the electricity provider Enron and Dynergy are accused of colluding to restrict the supply of electricity and gas to the Californian market in 2001 and thereby causing within the region (1) an infamous year of perennial brownouts, (2) falsely high prices for electricity, and (3) a build up of newly-built power plants that are now not needed and bankrupt. Enron and Dynergy oligopolisticly colluded to manufacture these false electricity shortages, so as to drive up electricity price and consequently profits [11]. Enron admitted to these claims in October 2002 [12]. A rigorous analysis of the UK electricity market has led to similar conclusions about the collusive activities of its generators in 1990s [13]. In these three ways, these instantaneous disparities between electricity supply and demand can create large peaks and troughs in the instantaneous electricity price.

Figs. 5 and 6 show the hypothetical aggregate supply and demand curves for electricity in England. As previously mentioned, electricity demand is inelastic (insensitive to changes in price); however, electricity supply is price elastic (sensitive). Fig. 5 characterises the price of electricity over the long-run (over a period of days or longer). Because lead times for demand are long enough, the full spectrum of electricity suppliers may enter the market and the resulting

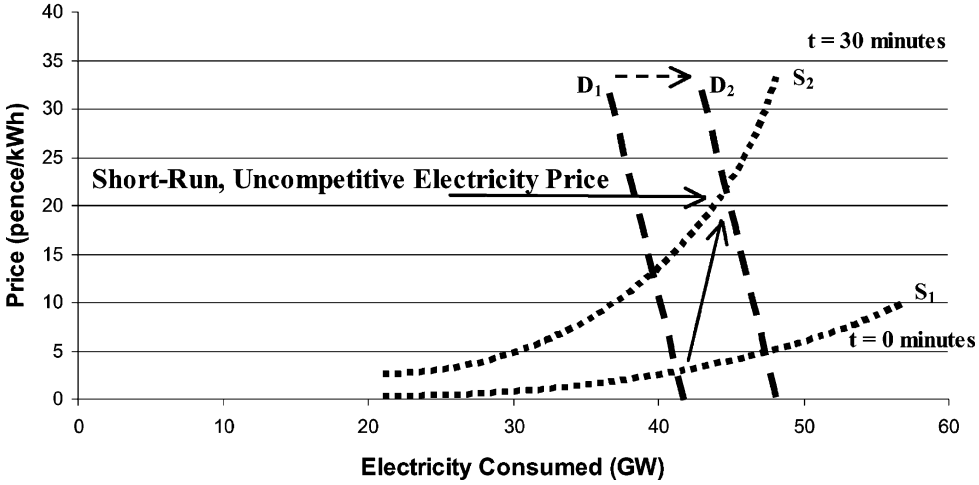

Fig. 6. The aggregate supply and demand for electricity in England in the short-term. In the short-term, electricity markets achieve a stable equilibrium between supply and demand at a relatively high, uncompetitive price.

electricity price is relatively low. Fig. 5 characterises an electricity market that

(1) has a large portion of electricity generators competing to supply electricity,
(2) has reached a semi-competitive equilibrium, and
(3) therefore has a relatively low electricity price.

Fig. 6 characterises the price of electricity over the short-term (over a period of seconds, minutes, or hours). Fig. 6 characterises an electricity market that

(1) has a small portion of electricity generators competing to supply electricity,
(2) has reached an uncompetitive (unstable, short-term) equilibrium, and
(3) therefore has a relatively high price.

At time $t = 0$ min, the demand and supply for electricity is as it is in Fig. 5, at a long-term equilibrium. At time $t = 30$ min, the demand for electricity increases (from D_1 to D_2) but the number of suppliers who can rapidly respond to this change in demand is few, such that the supply of available generators simultaneously contracts (from S_1 to S_2). Essentially, the supply curve for delivering ''instantaneous'' and especially unscheduled power in the short-term (shown as S_2) takes a different shape. Compared with the original supply curve (shown as S_1) for long-term power, this new supply curve is more inelastic and has contracted in shape. As a result, after an instantaneous change in demand, because (1) the nature of electricity demand is inelastic, and (2) the supply has also simultaneously contracted, the price of electricity spikes. The price moves from the intersection of D_1 and S_1 not to the intersection of D_2 and S_1 (as under more normal supply conditions) but to the intersection of D_2 and S_2 because supply has also simultaneously contracted (or, rather, because the shape of the supply curve for this market segment—''instantaneous supply''—takes a more contracted shape.) The net result of these rapid instantaneous changes in demand is a series of price spikes, occurring many times through out a single day. These price spikes are similar to an oil shock (a rapid contraction in supply in the face of inelastic demand), occurring several times in a day.

Fig. 7 reproduces the supply and demand curves of Figs. 5 and 6 with an overlay of data from England's electricity market. The perennial spiking effect results in a wide distribution of values for combinations of consumption and price. The data show the band (or range) through which the supply curve shifts.

In comparing electricity market behaviour over the long and short-term, one can make an analogy with chemical systems: over long time periods, market mechanisms have time to reach a stable equilibrium, much like chemical systems do when the kinetics of the reaction are fast enough. By contrast, over short time periods, market mechanism reach unstable equillibria marked by a lack of competition and inflated prices (economic inefficiency), much as chemical systems with slow kinetics are marked by a failure to minimise the Gibbs free energy of the system (thermodynamic non-equilibrium).

This particular technical and economic nature of electricity markets results in a significant economic inefficiency. The economic inefficiency is quantitatively related to the financial difference between a competitive electricity price and the actual short-term, uncompetitive one (for example see [14]). In the example of Fig. 6, this financial difference is the vertical distance between the uncompetitive electricity price shown at the intersection of D_2 and S_2 and the competitive price shown at the intersection of D_2 and S_1. Economic inefficiencies are net losses to all actors in an economy (consumers, industry, and governments); economic inefficiencies are less when competition is greater; competition is greater when the barriers are low for suppliers to enter and exit a market. Economic inefficiencies are

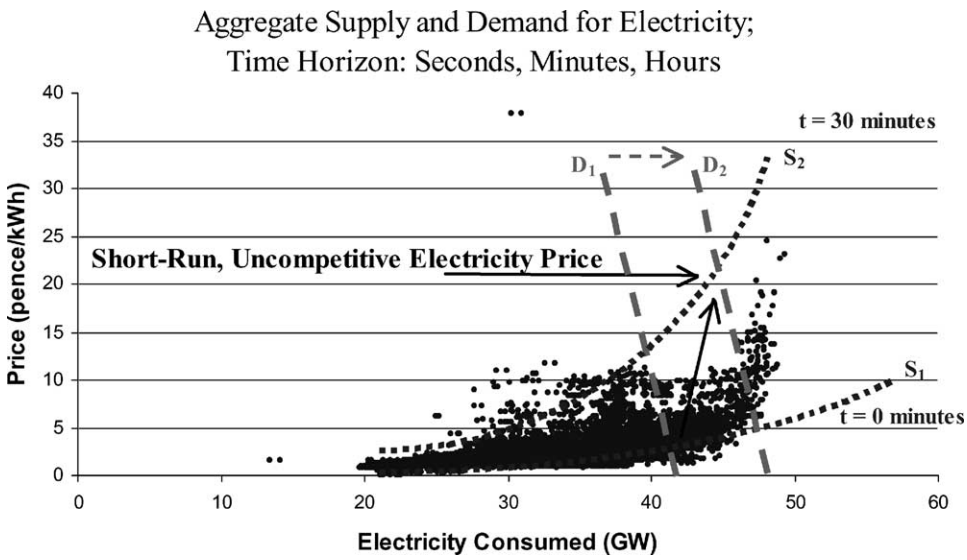

Fig. 7. An overlay of data from England's electricity system. England's electricity price and consumption data concurs with the behaviour of electricity markets described above.

prevalent in the electricity industry, because of one such barrier to entry: the large lag-time for power plants to change their power output levels. Therefore, a power generation device (or network of devices) that can reduce this lag-time in response can also reduce the extent of this market inefficiency. A greater supply of flexible power generators, able to rapidly respond to changes in demand, essentially allows the supply curve S_2 shown in Fig. 6 to shift out again towards the curve S_1 and towards a more competitive equilibrium. Power generators that are able to develop the ability to respond flexibly to changes in demand gain access to one of the most profitable market segments of the power industry. In turn, their entrance stands to benefit society by increasing competition in this market and decreasing prices. One such potentially flexible power generation technology is a network of combined heat and power (CHP) fuel cell systems (FCS).

1.1.1.2. Environmental inefficiencies due to high volatility in electricity demand. As shown in Table 1, electricity markets exhibit a high volatility in demand that not only causes economic inefficiencies, but also environmental ones. Due to the volatility of demand in electricity markets, excess electricity that is unexpectedly not needed in the last instance is dumped. Volatility in demand combined with more slowly responding electricity supply leads to periodic overproduction and consequent dumping of electricity, thereby incurring an incrementally greater amount of pollution than needed. In addition, the environment suffers from the marginally greater pollution incurred by meeting peaks in electricity demand, which often involves switching on the most polluting generating plants (typically old oil plants). Those few suppliers that are able to enter the market for instantaneous changes in electricity supply are among the most polluting.

1.1.2. Conventional generation suffers from dual economic and environmental inefficiencies because heat is produced but not usefully consumed

1.1.2.1. Economic inefficiencies because conventional generators produce heat that is not usefully consumed. As shown in Table 1, conventional power generators typically dispose of their heat by releasing it to the environment. Because generators usually dispose of this heat rather than sell it, the economy suffers from a dead-weight social loss (an economic inefficiency). If made available to them in a useful manner, customers would want to buy the waste heat from power generators, but, in most case, they cannot. Anytime a product is created, and customers would like to purchase that product but cannot, the economy incurs an economic loss (for example see [15]).

1.1.2.2. Environmental inefficiencies due to heat produced but not consumed. As shown in Table 1, conventional power generators typically dispose of their heat by releasing it to the environment, and this creates not only an economic inefficiency but also an environmental one. The environmental inefficiency is characterised by the degree of environmental impact (including pollution and green house gas emissions) created from heat produced but not usefully consumed. For example, in Germany, with its current mix of electricity generating plants, and a relatively modern transmission and distribution network with a 94.5% efficiency [16], the overall electrical efficiency of the power network was only 36% in 1999, with the majority of the remaining 64% released to the environment as waste heat, not usefully consumed [17]. That said, when discussing a technology under development, it is fair to compare this new technology not against current technology, but against a projection of current technology at

a point in the future when the new technology might conceivably enter the market. One starting point for this analysis is to derive the efficiency of a power network composed of modern versions of today's least expensive technologies [18]. As in 2001, the most inexpensive and fastest growing forms of power generation were combined cycle gas turbines (CCGTs) for base load and open cycle gas turbines (OCGTs) for peak load [19]. As in 2001, the most modern designs of each of these currently achieve electrical efficiencies of 58 and 38%, respectively. Based on an analysis of the average cost of electricity from each of these sources for different load factors, a Dresdner Kleinwort Benson study indicated that the optimal (most profitable) mix of these plants is approximately nine to one, respectively [20]. Therefore, the overall efficiency of such a future power generation, transmission, and distribution network is 53%, still with a large portion of the remaining 47% of the chemical energy of the fuel wasted as heat, not usefully consumed. Furthermore, the environment suffers a double, negative impact with heat production: first, from the thermal energy wasted by conventional centralised power generators; and second, from the energy wasted by onsite boilers and furnaces needed to create heat onsite (to serve the heat demand that could have been served by the simultaneous electricity generation process).

It is noteworthy that the economics community regards negative environmental impacts such as pollution as a source of economic inefficiency (for example see [21]). In some cases, the price of a particular product may not include the total cost to society of the pollution created during that product's manufacture [22]. When the price of a particular product does not fully incorporate all of the costs of creating that product, economists regard this occurrence as a failure of the free market. When consumers purchase such a product, they are not paying the full cost of the creation of that product (including the cost of the pollution). As a result, consumers pay less than the economically efficient price of that product (which would include the costs of pollution) and consume more of this product than the economically efficient quantity. When the price of a product does not fully incorporate the cost of its environmental impact, this failure of the free market acts to cross-subsidise consumption of this product above the economically efficient consumption level.

1.1.3. A more economically and environmentally efficient operating point uses a network of flexible, distributed CHP power generators

A more environmentally and economically efficient operating point for an electricity system can be achieved by operating a network of embedded generators such that there is a closer match between electricity (and heat) demanded with that supplied. For electricity (and heat) supply to more closely match electricity demand, electricity generators must achieve a quicker response time to changes in load. They must also deliver their waste heat to a useful thermal sink. These goals may be achieved best not by conventional generators but by a network of distributed combined heat and power (CHP) fuel cell systems (FCS) [23]. CHP FCS may achieve a competitive advantage over conventional generators if some of their inherent technical qualities are more fully developed in the research and development process. As mentioned previously, these inherent technical qualities include (1) an ability to vary their electrical load rapidly, (2) an ability to vary their heat to power ratio during operation to more closely match the thermal and electrical power supplied with that demanded, and (3) an ability to deliver their waste heat to a useful thermal sink [24]. Although at a nascent stage of development, these technical qualities of fuel cell systems exist, and, if further developed, could be the source of their competitive advantage over other power generation technologies. However, for fuel cell systems to more fully develop these technical qualities, the fuel cells industry must shift its research and development paradigm, from a historical focus on achieving high electrical efficiency [25] to a more forward focus of achieving high overall (electrical and thermal) efficiency. This article focuses on developing the last of these three inherent technical qualities: a fuel cell system's ability to deliver its waste heat to a useful thermal sink.

1.2. Combined heat and power fuel cell system thermal loop analysis

This article evaluates the CHP FCS shown in the schematic diagram of Fig. 8. This CHP FCS produces 6 kW of gross electrical power and 8 kW of useable heat for a building. This CHP FCS converts natural gas into electrical and thermal energy via four sub-systems. The four main subsystems are (1) the fuel processing sub-system, (2) the fuel cell sub-system, (3) the power electronics sub-system, and (4) the thermal management sub-system. The fuel processing sub-system reforms natural gas fuel into a hydrogen rich gas using an auto-thermal fuel reformer, such that the energy released from the exothermic partial oxidation of natural gas is equal to the energy consumed by the endothermic steam reforming of natural gas [26]. Downstream from the fuel processor, the fuel cell sub-system then uses a proton exchange member (PEM) fuel cell stack to convert the hydrogen rich gas into direct current (dc) electricity. Downstream of the fuel cell sub-system, the power electronics sub-system converts the dc electric power into alternating current (ac) power and manages the electrical current draw from the system against that drawn from the surrounding local electricity network. In conjunction with the fuel processing and fuel cell sub-systems, the thermal management sub-system captures waste heat from both of these subsystems for space and hot water heating. Through these four sub-systems, the 6 kWe CHP FCS provides electricity and heat.

The 6 kWe CHP FCS is evaluated under different scenarios so as to achieve an optimal thermal management subsystem. The thermal loop is evaluated for four different

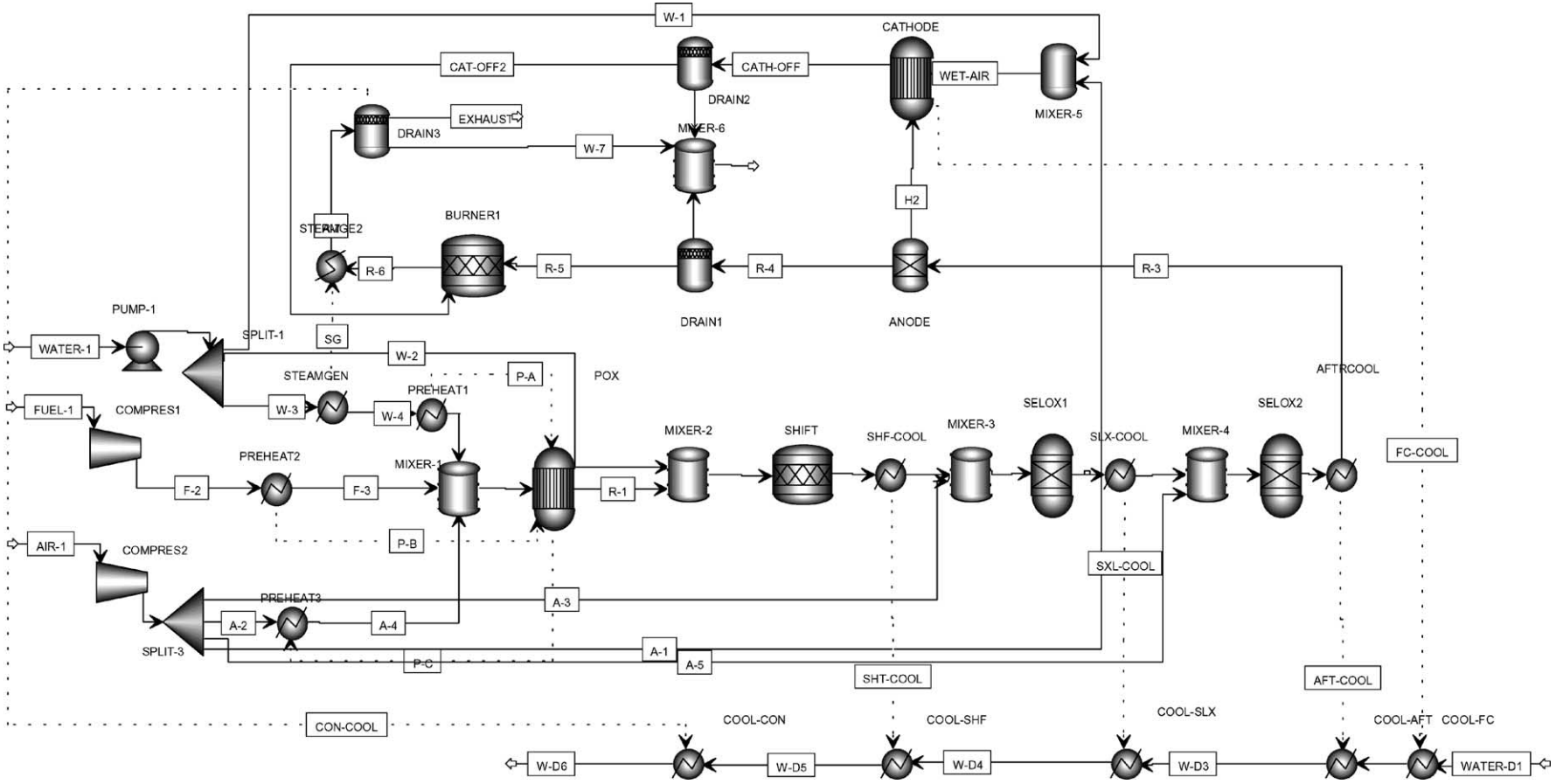

Fig. 8. Datum design condition: combined heat and power fuel cell system configuration.

physical configurations. These configurations are analysed by applying the technique of Pinch Point Analysis, which minimises the energy requirements for a process plant, to the fuel cell system [27]. The primary goal of Pinch Point Analysis is to optimise the overall heat recovery within a process plant by minimising the need to supply additional heating and/or cooling (for example see [28,29]). In an ideal Pinch Point Analysis solution, hot streams are used to heat cold ones and vice versa, with a minimum amount of additional heat transfer from an external source. External transfer decreases energy efficiency and profitability. The Pinch Point Analysis is based on a the results from running a computer model of the fuel cell system in the chemical engineering modelling program Aspen Plus®. This article discusses the results of the Pinch Point Analysis for the heat exchanger network around the fuel cell and the fuel processing sub-systems.

First, this article delineates the specifications for the 6 kWe system. Second, based on these design conditions, it discusses the results of the analysis from four different possible cooling loop configurations, with particular attention to the position of the condenser. Finally, it concludes that one of these four possible configurations provides optimal performance.

2. Experimental: modelling methodology and datum design conditions

2.1. Modelling methodology

2.1.1. Modelling tools

The analysis of CHP FCS thermal loop is based on a computer process model of a complete stationary fuel cell power plant producing a gross electrical power output of 6 kW. The model uses a combination of computer programs and languages: (1) Aspen Plus® steady-state chemical engineering process software version 11.1, (2) Microsoft Excel™, (3) Fortran, and (4) Microsoft Visual Basic™.

2.1.2. Modelling design objectives

The CHP FCS's heating loop should achieve certain design objectives, including five key design success factors: (1) high total thermal energy (and liquid water) capture, (2) simplicity of design, (3) simplicity of control, (4) low cost construction, and (5) low danger of temperature cross-over (maximize the pinch point temperature). The analysis discusses four configuration options for the cooling loop with respect to these five key design success factors.

This analysis investigates four options for configuring the cooling circuit, with particular attention paid to the condenser. The condenser is important to the overall system design because (1) it spans the largest temperature range of all thermal sources, (2) it produces as much heat as all the other thermal sources combined, and (3) it condenses out a certain amount of water which impacts the overall system's water balance. Therefore, the configuration of the condenser is one of the primary design options to address.

2.2. Datum design conditions

The fuel cell system is initially evaluated around a certain datum design condition. This datum design condition is based on (1) a particular system configuration, (2) particular operating specifications, and (3) particular assumptions, delineated as follows.

2.2.1. Datum design condition system configuration

The datum design condition is based on a specific system configuration with thermal sources and sinks. The fuel cell system has five primary thermal sources that require cooling by an external source. These five primary sources are (1) the fuel cell, (2) the aftercooler, (3) the selox reactor, (4) the post-water-gas-shift stream, and (5) the condenser. The fuel cell system has one primary external thermal sink, the domestic water cooling loop, which provides hot water and heating for the building. The five primary thermal sources and one external sink are shown in Fig. 8. The five sources are labelled right to left in the same order: (1) COOL-FC, (2) COOL-AFT, (3) COOL-SLX, (4) COOL-SHF, (5) COOL-CON, and the one sink is the stream passing through these labelled WATER-D1.

2.2.2. Datum design condition operating specifications

The datum design condition is based on a collection of particular operating specifications, set at a constant fuel flow rate that is equivalent to 6 kWe gross fuel cell stack output.

2.2.2.1. Datum design condition operating specifications for the overall system. At full power, the overall system operates with a high net system electrical efficiency (LHV) of 35.5% [WC1] and a resulting system heat to power ratio (net heat to net electrical power) of 1.34. The fuel cell subsystem operates with a high gross electrical efficiency of 61.0% [WC2]. Approximately 17% of the LHV fuel energy is lost from the system as heat in the uncooled and uncondensed cathode and anode exhaust gas streams exiting at 65 °C.

2.2.2.2. Datum design condition operating specifications for the fuel cell sub-system [30]. As shown in Table 2, the Aspen Plus® computer model of the CHP FCS is based on experimental data from a fuel cell stack manufacturer. The fuel cell stack produces 6 kW of electrical power at an operating temperature of 70 °C.

2.2.3. Datum design condition operating specifications for the fuel processor sub-system

As shown in Table 3, the Aspen Plus® computer model of the CHP FCS is also based on experimental data from a manufacturer's fuel processor. Through a series of catalytic chemical reactors, the fuel processor converts natural gas fuel typically composed of 97% methane into a reformate

Table 2
The Aspen Plus® computer model is based on experimental data from a fuel cell stack manufacturer

Fuel cell stack sub-system specifications	
Gross fuel cell stack electrical output (W)	6031
Anode stoichiometery	1.40
Anode utilisation	0.714
Cathode stoichiometery	2.0
Cathode utilisation	0.5
Cathode inlet relative humidity (%)	75
Anode inlet relative humidity (%)	100
Stack operating temperature (°C)	70.0
Net water diffusion (moles H_2O diffuse/H_2 react)	0.32
Cathode inlet pressure (bar_abs)	1.15
Anode inlet pressure (bar_abs)	1.02

gas typically composed of 33.5% H_2O, 33% H_2, 11% CO_2, 0.5% CH_4, 22% N_2 and a few ppm CO (molar).

2.2.4. Datum design condition operating specifications for the thermal management sub-system

The datum design condition assumes that the external thermal management system is composed of five thermal sources that exchange heat with 100% efficiency with a single sink, the domestic cooling loop. These five thermal sources are shown schematically in Fig. 8. These five thermal sources are arranged in series according to their temperature differentials. As shown in Table 4, the anode and cathode off-gas passes through an isothermal condenser at 65 °C. The domestic cooling stream inlet temperature is the same as that of mains temperature water, 25 °C, and the outlet temperature is the standard for most British and European households, 80 °C. The flow rate of the domestic cooling loop is varied to achieve this outlet temperature.

Table 3
The Aspen Plus® computer model is based on experimental data from a manufacturer's fuel processor

Fuel processor sub-system specifications	
Actual fuel to air ratio	0.43
Stoichiometric fuel to air ratio	0.50
Equivalence ratio	0.9
Steam to carbon ratio	3.09
Fuel flow rate (mol/min)	1.23
Lower heating value equivalent of fuel flow (W)	16578
Moles of H_2 produced/moles fuel supplied	2.77
Fuel composition (molar fraction)	
CH_4	0.9674
C_2H_6	0.0164
C_3H_8	0.0019
C_4H_{10}	0.0005
C_5H_{12}	0.0002
O_2	0
N_2	0.0045
H_2O	0
CO	0
CO_2	0.0091
H_2	0

Table 4
The Aspen Plus® computer model is based on experimental data for domestic cooling loops based on water circulation inside British homes

Thermal management sub-system specifications	
Condenser outlet temperature (°C)	65
Domestic cooling stream inlet temperature (°C)	25
Domestic cooling stream outlet temperature (°C)	80
Heat exchanger efficiency (%)	100
Heat exchanger type	Simple
Domestic cooling stream flow rate	Variable

Table 5 summarises these specifications for the five thermal sources and the one sink. Table 5 specifies each thermal source's name as shown in Fig. 8, its description relative to the CHP system, its initial thermal state (either hot or cold), its heat flow capacity (the product of mass flow and specific heat capacity), its temperature differential, and its heat load (the amount of energy transferred to or from the stream). As highlighted in Table 5, the domestic cooling loop water enters the fuel cell system from the outside at a temperature close to ambient (assumed to be 25 °C for the datum design condition) and must be heated to a temperature useful for the hot water needs of a building (assumed to be 80 °C for the datum design condition). Also, as highlighted in Table 5, the outlet temperature of the condenser is 65 °C. At this condenser outlet temperature, if all of the heat is captured upstream of the condenser, this amount constitutes a thermal efficiency (defined as the energy available as useful heat in terms of the total chemical energy of the fuel) of 43.4% based on the LHV of the fuel. This is the maximum thermal efficiency at this condenser outlet temperature. This condenser outlet temperature leads to a slight water imbalance of 1.43 mol/min of net water that must be added to the system.

2.3. Datum design condition assumptions

The datum design condition is based on several assumptions. First, it assumes that all the sub-system's heat exchangers are 100% efficient counter-current heat exchangers with zero pressure drop. The primary advantage of counter-current exchangers is the higher outlet temperature of the cold stream, which can be hotter than the outlet temperature of the hot stream (but not its inlet). The assumption of 100% efficient heat exchangers indicates, for example, that all of the heat released by the reaction of hydrogen and oxygen at the fuel cell is absorbed by the cooling loop. Second, the datum design condition assumes that the cooling loop is composed entirely of the domestic water cooling loop, without any secondary cooling loops in between, such that the gas streams of the fuel processing and fuel cell sub-systems exchange heat directly against the domestic water

Table 5
Datum design condition: operating specifications for thermal sources and sinks

Label name	Thermal source/sink	Description	Initial thermal state	Heat flow capacity, MC_p (kW/K)	Supply temperature, T_{in} (°C)	Target temperature, T_{out} (°C)	Heat load, Q (watts)
COOL-FC	Fuel cell stack	Heat released from the electrochemical reaction of hydrogen and oxygen	Hot	NA	70	60	2762
COOL-AFT	Aftercooler	Heat extracted from the reformate stream after the selox and before the fuel cell	Hot	23	108	70	863
COOL-SLX	Selox	Heat extracted from the reformate during the exothermic selective oxidation reaction	Hot	6	126	100	151
COOL-SHF	Post-shift	Heat extracted from the reformat after the shift reactor, before the selox reactor	Hot	6	260	117	825
COOL-CON	Condenser	Heat released from condensing water out of the anode and cathode exhaust gases	Hot	22	219	65	3370
WATER-D1	Domestic cooling loop	Domestic water cooling loop exchanging heat between fuel cell system and building	Cold	145	25	80	7971

cooling loop. The only exception to this is the fuel cell, which requires a secondary intermediate loop composed of an equal ratio of deionised water to ethylene glycol by volume. Both this intermediate fuel cell loop and the domestic cooling loop must operate above certain minimum flow rates so as to avoid vaporisation of the cooling fluids [31]. Finally, to achieve the target outlet domestic cooling loop temperature (set at 80 °C for the datum design condition), the datum design condition assumes that the mass flow rate of the cooling loop water is varied. Where the domestic cooling loop is separated into parallel streams and then recombined, the temperature of at least one of these parallel streams may significantly exceed the datum design condition outlet temperature before being recombined; this configuration is limited only by the cooling fluid's vaporisation temperature.

3. Results and discussion: analysis of domestic cooling loop configurations

Based on the above datum design conditions, this analysis investigates four different configuration options for the cooling circuit. These four different design configuration options primarily investigate the position of the condenser, one of the primary thermal sub-system design considerations. The condenser captures heat from the anode and cathode off-gases. The condenser is the thermal source that has the greatest danger of creating a temperature crossover as it spans the widest temperature range (from 65 to 219 °C, as shown in Table 5) and, in so doing, crosses the temperatures ranges of all of the other four thermal sources. At the same time, it is important to capture a majority of the condenser's energy available because this component is by far the largest single thermal source, producing over half the heat available in the entire system. In the process of energy capture, the condenser is also converting water vapour from the anode and cathode off-gases into liquid water. This liquid water needs to be reused in other parts of the CHP FCS to obtain a neutral system water balance. For this reason, the condenser is also very important to the overall system design because the degree to which it condenses anode and cathode exhaust gas water impacts on the overall system's water balance. Therefore, the position of the condenser is one of the primary detailed design configuration options to address. This analysis investigates four options for configuring the cooling circuit, with particular attention to the condenser. The analysis discusses these four configuration options with respect to six key design success factors.

3.1. Domestic cooling loop configuration options

The four different options for configuring the cooling circuit are shown in Fig. 9. As shown in Fig. 9, Configuration 1 orders the five thermal sources in series, with a single condenser (shown as a shell and tube heat exchanger) at the end of this loop. Configuration 2 orders the five thermal sources also in series, but splits the single condenser into five separate condensers (shown as a shell and tube heat exchanger) that are interspaced between the other four thermal sources. Configuration 3 places the four thermal sources in series with respect to each other and altogether in parallel with respect to a fifth thermal source, the condenser (shown as a shell and tube heat exchanger). Finally, Configuration 4 is identical to Configuration 3, with one exception: the single condenser is split into two separate condensers (shown as a shell and tube heat exchanger), with the first stage at the entrance to the cooling loop.

3.2. Evaluation of four domestic cooling loop configuration options

Table 6 compares and contrasts these four cooling loop options in terms of five key design success factors. These five key design success factors include (1) a high level of total energy captured from the fuel cell system into the

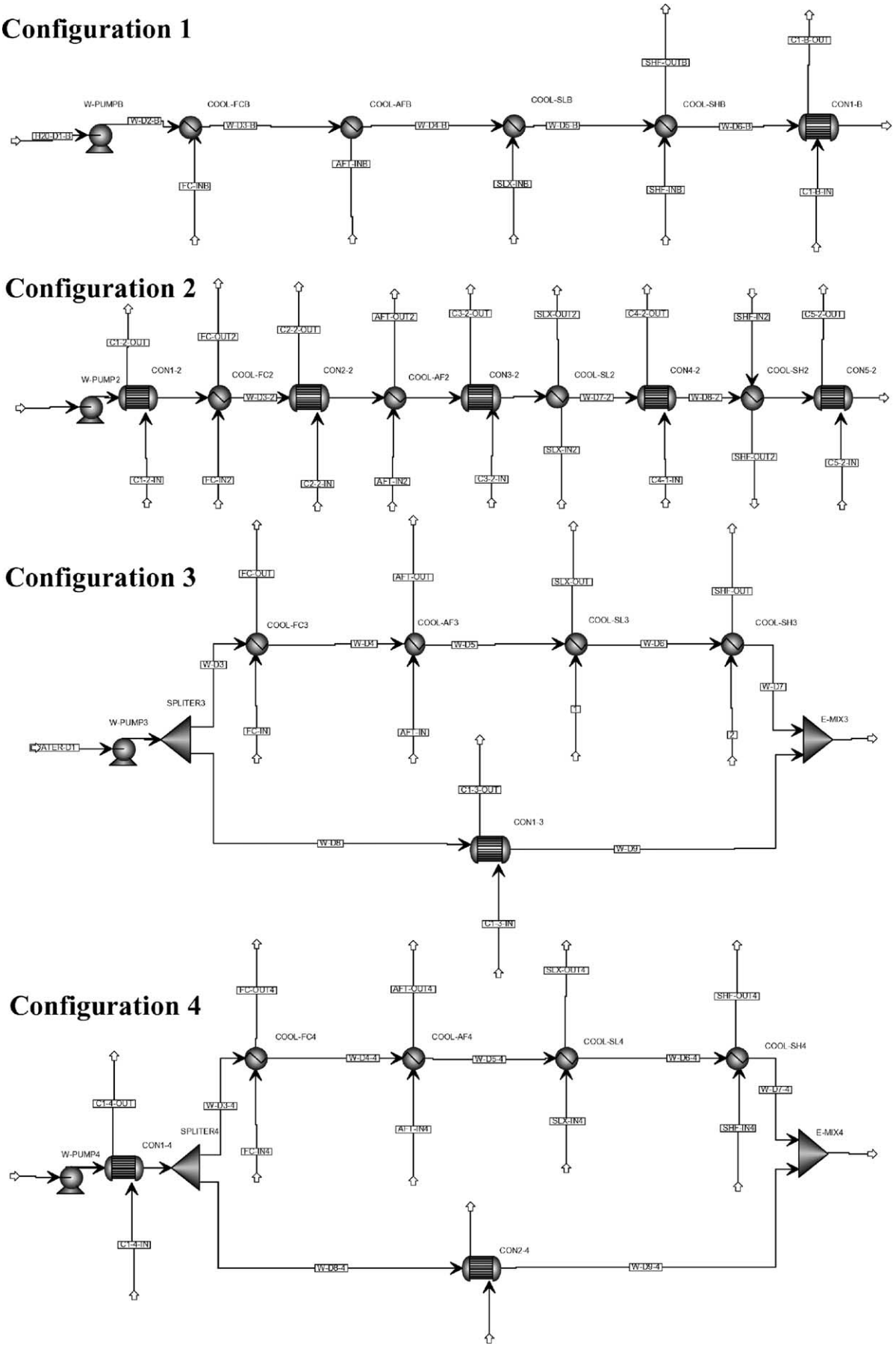

Fig. 9. Four possible configurations for the domestic cooling loop.

Table 6
Comparison of four cooling loop configurations against five key design success factors

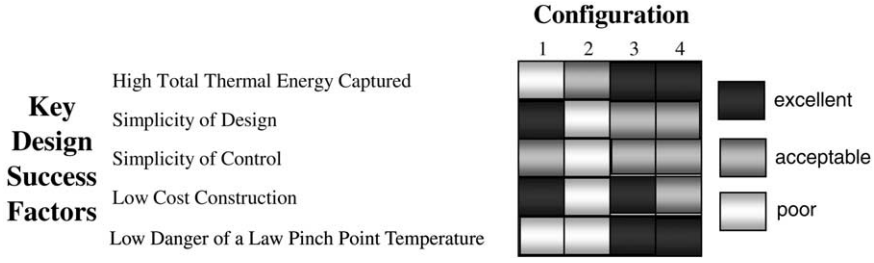

cooling loop, (2) the simplicity of the design of the cooling loop, (3) the simplicity of its control, (4) the low cost of its construction, and (5) a low danger of temperature cross-over (maximize the pinch point temperature). The first of these, the maximisation of energy capture, leads to another benefit: a larger amount of liquid water captured from the system, and therefore a higher likelihood of achieving neutral or positive system water balance. The last of these, creating a system with a low danger of temperature cross-over between streams, is synonymous with maximising the overall system's pinch point.

3.2.1. Configuration 1: Series thermal loop with partial condenser

The advantages and disadvantages of Configuration 1 are summarised in Table 6 in the first column. As shown in Fig. 9, Configuration 1 orders the five thermal sources in series, with a single condenser at the end of this loop. If all five thermal sources are arranged in series in a thermal loop, the condenser can only be configured at the end of this loop, because it would otherwise crossover the temperature regions of the other thermal sources, because of its large temperature range. As shown in Table 6, Configuration 1's main advantages are that (1) it has a simple design (shown in row two), (2) it has an acceptably simple control system (row three) with only one mass flow controller at the inlet, (3) it has a low cost construction due to a low number of components, the least of all the configurations presented (row four) with only five heat exchangers. Configuration 1's primary drawback is that it has a danger of a low pinch point temperature (row five). Fig. 10 shows that, with this configuration, a pinch point of 4 °C is encountered in the condenser, the last heat exchanger in the series. To this configuration's benefit, Fig. 10 shows that all the heat that is released by the five thermal sources can be captured. However, given the high danger of a low pinch point temperature, Configuration 1's second drawback is that, if temperatures of hot and cold condenser streams do cross-over, the system will have lower percentage of the total energy captured (row one), because the condenser's waste heat will not be entirely recovered. It is particularly dangerous to have such a low pinch point in the single system component most crucial for both heat recovery and water balance. As a result, other configurations must be considered.

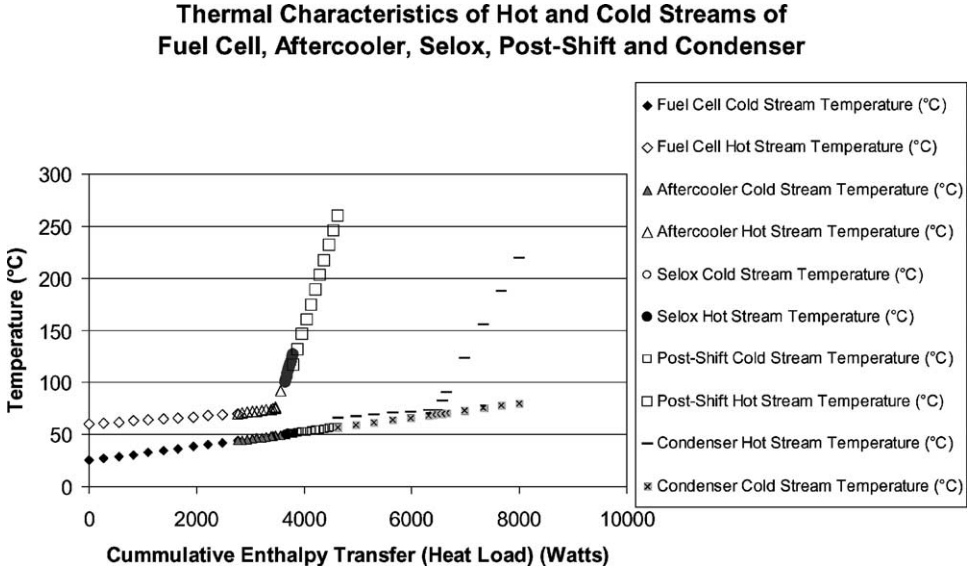

Fig. 10. Temperature approach within five thermal sources' streams, as a function of the change in enthalpy of those two streams. The pinch point is in the condenser at 4 °C.

3.2.2. Configuration 2: Series thermal loop with split condensers

The advantages and disadvantages of Configuration 2 are summarised in Table 6 in the second column. Configuration 2 orders the five thermal sources also in series, but splits the single condenser into multiple condensers that are interspaced between the other four thermal sources so as to maximize the pinch point temperature between streams for the amount of heat transferred. While this configuration (1) maintains the simpler physical series configuration (row two), and (2) captures a greater percentage of the heat available from the condenser than Configuration 1 (row one), the primary disadvantages of this configuration are the (1) much larger hardware requirements (several condensers instead of one) which increases the construction costs (row four), along with (2) a strong danger of a low pinch point temperature only mitigated with more complex design and control (rows five and three).

3.2.3. Configuration 3: Parallel thermal loop with single condenser

The advantages and disadvantages of Configuration 3 are summarised in Table 6 in the third column. Configuration 3 manages the cooling loop by placing four thermal sources in series with respect to each other and altogether in parallel with respect to a fifth thermal source, the condenser. While the disadvantages of this design are (1) its greater physical system complexity than Configuration 1 (row two), and (2) more complex control compared with Configuration 1 (row three), the primary advantages are (1) a smaller number of condensing stages and hardware as compared with Configuration 2 (row two), (2) its simpler control configuration as compared with Configuration 2 (row three), (3) its ability to capture 100% of the waste heat, under certain design conditions (row one), and (4) its ability to maximize the pinch point temperature (row five).

3.2.3.1. Analysis of pinch points for Configuration 3 at full power (6 kWe). Figs. 11 and 12 show the modelling results for Configuration 3, as a change in enthalpy versus temperature plot. The change in enthalpy refers to the aggregate level of enthalpy being exchanged between the hot stream and the cold stream, and the temperatures shown at each enthalpy point are the inlet and outlet temperatures for the thermal source. Fig. 11 shows the temperature versus enthalpy plot for the four thermal sources in series on one side of the parallel loop: the fuel cell, aftercooler, selox, and post-shift sources. Fig. 12 shows the temperature versus enthalpy plot for the condenser on the other side of the parallel loop. The combined total flow rate for both streams is the mass flow rate needed to capture all the heat available so as to increase the initial inlet temperature for the domestic cooling stream from 25 °C to the desired outlet temperature of 80 °C. The flow rates chosen for each of the streams in parallel are based on the mass flow ratio of 0.58 (first parallel stream) to 0.42 (second parallel stream), which allows each parallel stream to independently achieve an exit temperature of 80 °C. Figs. 11 and 12 show each parallel stream's pinch point temperature, the minimum temperature difference between hot and cold streams for effective heat transfer. Fig. 11 highlights the first parallel stream's pinch point temperature at approximately 3500 W cumulative heat load in the aftercooler with a value of 8 °C. Fig. 12 highlights the second parallel stream's pinch point temperature at approximately 1800 W cumulative heat load in the condenser with a value of 18 °C.

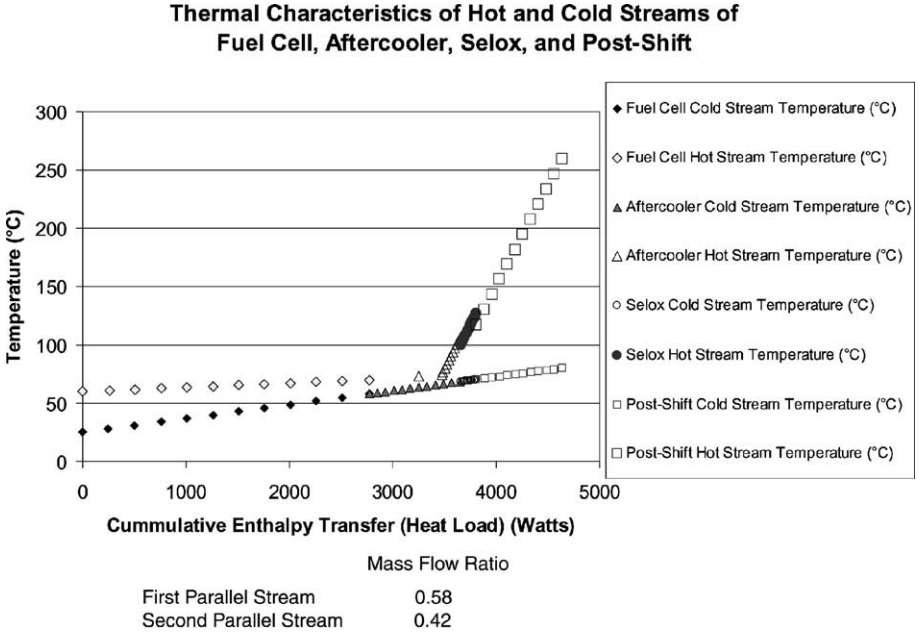

Fig. 11. Temperature approach within four thermal sources' streams, as a function of the change in enthalpy of those two streams. At 6 kWe rating, the pinch point is in the aftercooler at 8 °C.

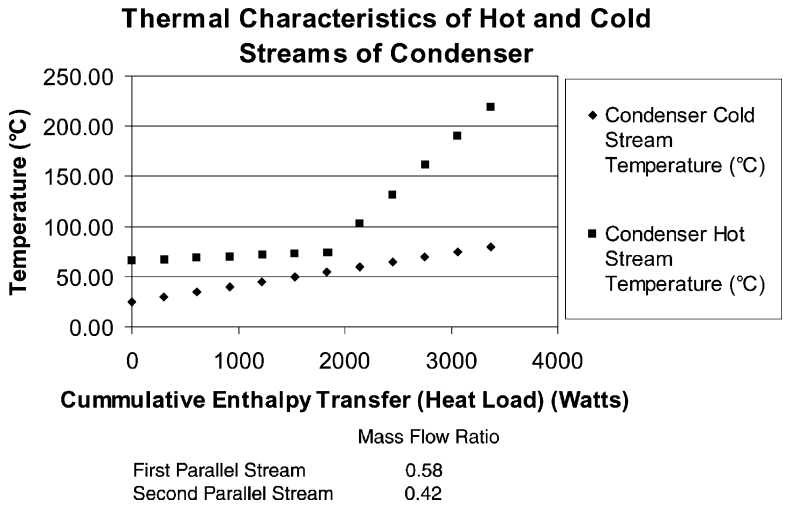

Fig. 12. Temperature approach within condenser's heat exchanging streams, as a function of the change in enthalpy of these two streams. The condenser's minimum temperature approach is 18 °C.

Keeping the combined total mass flow rate of water to the domestic cooling loop constant at the same rate, the ratios of the flows in the two parallel branches were varied to find the mass flow rate ratio where the pinch point in the system could be maximised (and the danger of cross-over minimised). Fig. 13 shows the results of this analysis, by plotting the minimum pinch point temperature for each thermal source with respect to the ratio of mass flow of the first parallel stream (containing the fuel cell, aftercooler, selox, and post-shift) with respect to the total flow rate. As shown in Fig. 13 by the intersection of the aftercooler pinch point curve and the condenser pinch point curve, the pinch point for the system can be maximised to a temperature difference of 12.5 °C by operating at a mass flow ratio of 0.64. If the mass flow ratio range is maintained between 0.60 and 0.67, the pinch point temperature will fall at or above 10 °C. At one extreme, the flow ratio is limited to above a certain minimum by the pinch point in the aftercooler (shown by the square symbols) to avoid a temperature cross-over in the aftercooler's hot and cold streams. At the other extreme, the flow ratio is limited to below a certain maximum by the pinch point in the condenser (shown by the starred crosses), because the condenser's cooling water must remain below 100 °C to avoid vaporisation. The composite sketch of the system's overall pinch point range is shown as the overall pinch point curve (shown by a single curve), which is the composite minimum of the aftercooler pinch point and condenser pinch point curves.

3.2.3.2. Overall heat-transfer coefficient and heat exchanger area for Configuration 3 at full power (6 kWe). For heat exchangers in the domestic cooling loop, their overall heat-transfer coefficient U (a composite description of the convective, conductive, and radiative resistance for a particular geometry of heat exchanger) is dominated by the convective resistance of the gaseous fluid ($1/hA$), which is much larger than that of the liquid fluid or the conductive resistance.

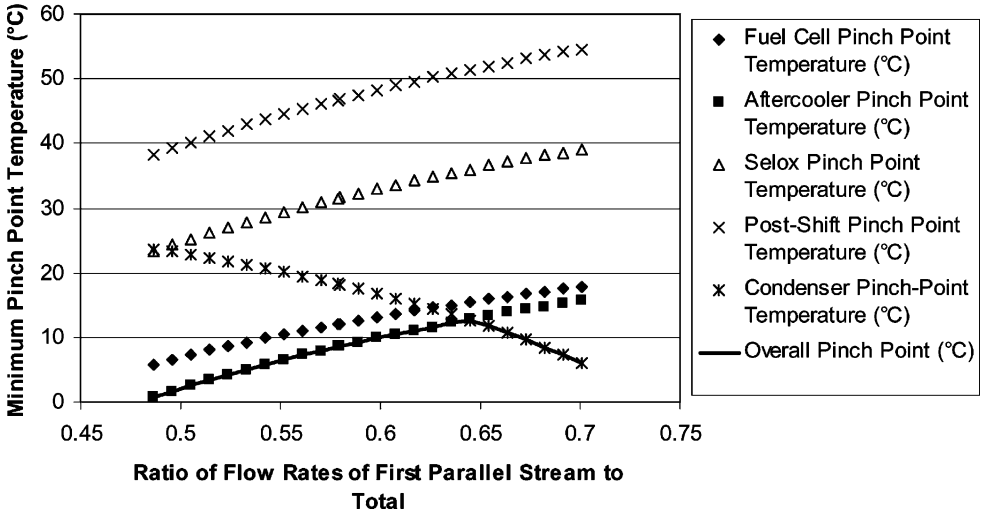

Fig. 13. Analysis of pinch points within all five thermal sources of the domestic cooling loop, as a function of flow rate to the two parallel streams. The system's pinch point can be maximised to 11 °C by controlling the ratio of flow rates to the two parallel streams. Results for 6 kWe.

The overall heat-transfer coefficient U and the heat exchanger's surface area A are calculated from the inlet stream conditions. First, the outlet temperature of the cold domestic cooling stream (T_{c_2}) is calculated based on simple energy balance for a counter-current flow heat exchanger, such that

$$T_{c_1} = T_{c_2} - \frac{q}{m_c c_c} = T_{c_2} - \frac{m_h c_h (T_{h_1} - T_{h_2})}{m_c c_c},$$

where T_h and T_c are the temperatures of the hot and cold streams, respectively, with the numbers 1 and 2 referring to the inlet and outlet, respectively; q is the heat transfer from the hot stream to the cold stream; and m and c are the mass flow rates and heat capacities of the hot (h) and cold (c) streams, respectively (for example see [32]). Second, with the inlet and outlet temperatures of all hot and cold streams, the log mean temperature difference (LMTD) (ΔT_m) is calculated, according to

$$\Delta T_m = \frac{(T_{h_2} - T_{c_2}) - (T_{h_1} - T_{c_2})}{\ln[(T_{h_2} - T_{c_2})/(T_{h_1} - T_{c_1})]},$$

where the log mean temperature difference is the mean temperature difference across the heat exchanger between the hot stream and the cold streams. Finally, U and A are back-calculated based on

$$q = UAF\,\Delta T_m,$$

where F is the correction factor that compensates for the geometrical difference between the actual heat exchanger and the standard counter-current flow concentric-pipe heat exchanger upon which the log mean temperature equation is based (for example see [33]). This last equation assumes that (1) the specific heats of the fluids are constant with temperature, and (2) the convection heat-transfer coefficient does not vary across the geometry of the heat exchanger. For this analysis, a double-pipe heat exchanger design was assumed; hence $F = 1$.

Based on the analysis for Configuration 3, Table 7 indicates the heat exchanger specifications for the five thermal sources. Table 7 indicates for each thermal source (1) the product of the heat transfer coefficient U and the heat exchanger area A for a range of values that deliver a system pinch point temperature greater than 10 °C, (2) a reasonable estimate of the heat transfer coefficient obtainable for that type of flow (1000 W/(m^2 °C) for liquid to liquid exchange and 40 W/(m^2 °C) for liquid to gaseous exchange), (3) based on these estimates for heat-transfer coefficient, the heat exchanger surface area needed, and (4) based on a compact heat exchanger design, assuming 650 m^2/m^3 [WC3] the resulting heat exchanger volume needed. Because these values for the product of U and A are calculated at the datum design condition of the system's highest fuel flow rate equivalent to 6 kWe gross fuel cell stack output, if the heat exchangers are slightly oversized in relation to these maximum values, at lower flow rates, these exchangers will still achieve the design heat transfer.

3.2.3.3. Analysis of pinch points for Configuration 3 at one-fourth full power (1.5 kWe). In addition to the analysis at the datum design condition of 6 kWe (the plant's maximum power output), Configuration 3 is also analysed at the power plant's minimum setting, 1.5 kWe. The 1.5 kWe plant was assumed to have a similar temperature profile across major system components as at the 6 kWe rating. This assumption is bolstered by experimental data attained for a 6 kWe fuel reformer. Although in reality, some portion of the system's heat losses will be constant with output, for simplicity, this model assumes that these losses vary in proportion to the output.

At 1.5 kWe, the system's maximum thermal efficiency (usable heat to fuel energy) and its degree of water imbalance are less than at 6 kWe. At this fuel cell power output setting, at the datum design condition condenser outlet temperature of 65 °C, if all of the heat is captured upstream of the condenser, this amount constitutes a thermal efficiency of 37.2% based on the LHV of the fuel (slightly less than the 43.4% efficiency at 6 kWe due to the higher electrical efficiency of the fuel cell at lower powers). At 1.5 kWe, this is the system's maximum thermal efficiency. At this setting, this condenser outlet temperature of 65 °C leads to the same proportion of water imbalance, such that 0.36 mol/min of net water that must be added to the system (following the 1:4 turn-down ratio in concurrence with the 1.43 mol/min deficit at 6 kWe).

Figs. 14 and 15 show the modelling results for Configuration 3, as change in enthalpy versus temperature plots,

Table 7
Heat exchanger specifications for the five thermal sources (6 kWe)

Thermal source	Product of heat-transfer coefficient (U) and heat exchanger surface area, A (W/°C)		Assuming max value of $U \times A$		
	Maximum	Minimum	Assumed heat-transfer coefficient, U (W/(m^2 °C))	Resulting heat exchanger surface area, A (m^2)	Heat exchanger volume for compact design (m^3)
Fuel cell	123.3	112.2	1000	0.12	0.00018
Aftercooler	68.7	52.6	40	1.52	0.00233
Selox	3.4	3.1	40	0.08	0.00012
Post-shift	8.2	7.7	40	0.20	0.00031
Condenser	94.7	117.0	40	2.65	0.00407

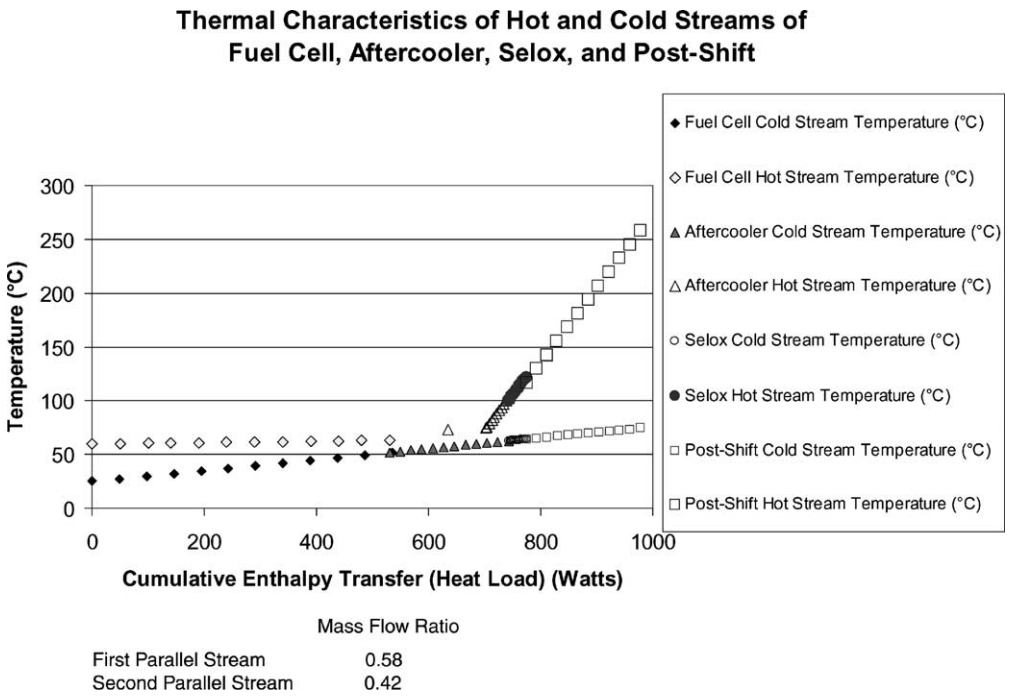

Fig. 14. At the 1.5 kWe rating, the pinch point is in the fuel cell at 11 °C.

similar to those of Figs. 11 and 12. As shown by a comparison of Figs. 11 and 14, the temperature profiles for the hot and cold streams follow the same general pattern at 6 kWe as at 1.5 kWe, though at a lower enthalpy range for 1.5 kWe. Although they follow the same general pattern, there is also an important difference: whereas the 6 kWe operation has its pinch point in the aftercooler at of 8 °C, the 1.5 kWe has a pinch point at the exit of the fuel cell at 11 °C. At the 1.5 kWe setting, by comparison, the minimum temperature approach in the aftercooler is 14 °C, well above the system pinch point. The system pinch point differs at the lower power setting because the fuel cell operates at a higher electrical efficiency at lower powers; consequently the fuel cell produces a lower contribution of waste heat for capture in the domestic cooling loop (37.2% of LHV at 1.5 kWe versus 43.4% at 6 kWe). As shown in Fig. 15, the minimum temperature approach in the condenser is the same as for the 6 kWe run, 19 °C.

Similar to the previous analysis, the total mass flow rate of water to the domestic cooling loop is kept constant while varying the ratio of the flows to the two parallel streams so as to maximise the system's pinch point temperature. Similar to Fig. 13, Fig. 16 shows the results of this analysis, by plotting the minimum pinch point temperature for each thermal source with respect to the ratio of mass flow of the first parallel stream with respect to the total flow rate. As shown in Fig. 16 by the intersection of the fuel cell pinch point

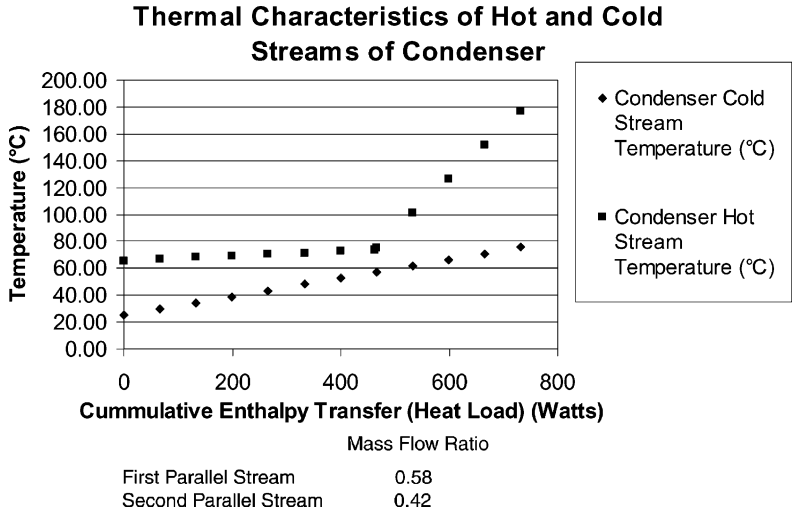

Fig. 15. At the 1.5 kWe rating, the minimum temperature approach in the condenser remains 19 °C.

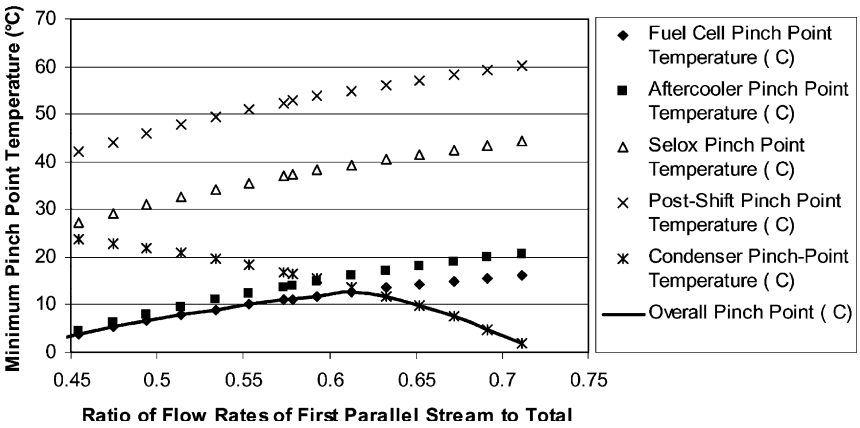

Fig. 16. Analysis of pinch points within all five thermal sources of the domestic cooling loop, as a function of flow rate to the two parallel streams. The System's pinch point can be maximised to 13 °C by controlling the ratio of flow rates to the two parallel streams. Results for 1.5 kWe.

curve and the condenser pinch point curve, the pinch point for the system can be maximised to a temperature difference of 12.7 °C by operating at a mass flow ratio of 0.61. The system may achieve a pinch point temperature at or above 10 °C by allowing the mass flow ratio range to be maintained between 0.58 and 0.65. At one extreme, the flow ratio is limited to above a certain minimum by the pinch point in the fuel cell, and at the other extreme, by the pinch point in the condenser. The composite sketch of the system's overall pinch point range is shown as the overall pinch point curve (shown by a single curve), which is the composite minimum of the fuel cell pinch point and condenser pinch point curves.

3.2.3.4. Overall heat-transfer coefficient and heat exchanger area for Configuration 3 (1.5 kWe). Following the same methodology as outlined in the previous section, the appropriate heat-transfer coefficients were determined for the five thermal sources at this lower power setting. As shown in Table 8, for all five thermal sources, the product of the heat-transfer coefficient U and the heat exchanger area A decreases by a factor of between four and five at the one-fourth power (1.5 kWe) setting.

3.2.3.5. Control system for Configuration 3. This parallel loop can be controlled in a few ways, with one of the more cost-effective strategies presented here. For a cost effective unit ready for commercial production, the parallel loop can be controlled using (1) a pump, (2) a diverter valve, (2) two thermocouples, and (3) a controller. As shown in Fig. 9 in Configuration 3 by the schematic pump "W-PUMP3", the pump is placed at the start of the cooling loop to control the loop's total mass flow rate. The diverter valve is also placed at the entrance of the cooling loop, shown in Fig. 9 in Configuration 3 at the location of the splitter "SPLITER3". Two thermocouples sense the temperature of the water in the two separate parallel loops. The controller receives input temperature readings from the two thermocouples, and outputs the desired mass flow rate to the pump and mass flow ratio to the diverter valve. Such a control system is depicted in the schematic diagram of Fig. 17. The thermocouples are shown (1) at the outlet of the condenser, and (2) between the aftercooler and the fuel cell, because these areas, as shown by the previous analysis have been the most susceptible to temperature crossover by having exhibited the system's minimum pinch point. The control strategy would be developed once the prototype system had been tested and used to validate the Aspen Plus® model. The aim of the control system is to use a minimum of transducers and actuators (so as to minimise the cost), but to rely on control laws being embedded in the controller that reflect the system operation (for example, to avoid local overheating for the fuel cell stack, there should be some circulating flow even during start-up, when one does not need cooling to an external loop for cooling the other components).

Table 8
Heat exchanger specifications for the five thermal sources (1.5 kWe)

Thermal source	Range for product of heat-transfer coefficient, U and heat exchanger surface area, A (W/°C)		Assumed heat-transfer coefficient, U (W/(m^2 °C)	Resulting heat exchanger surface area, A (m^2)	Heat exchanger volume for compact design (m^3)
Fuel cell	26.9	23.3	1000	0.03	0.000039
Aftercooler	13.5	10.2	40	0.30	0.000457
Selox	0.7	0.6	40	0.02	0.000025
Post-shift	2.0	1.8	40	0.05	0.000073
Condenser	21.8	28.3	40	0.63	0.000963

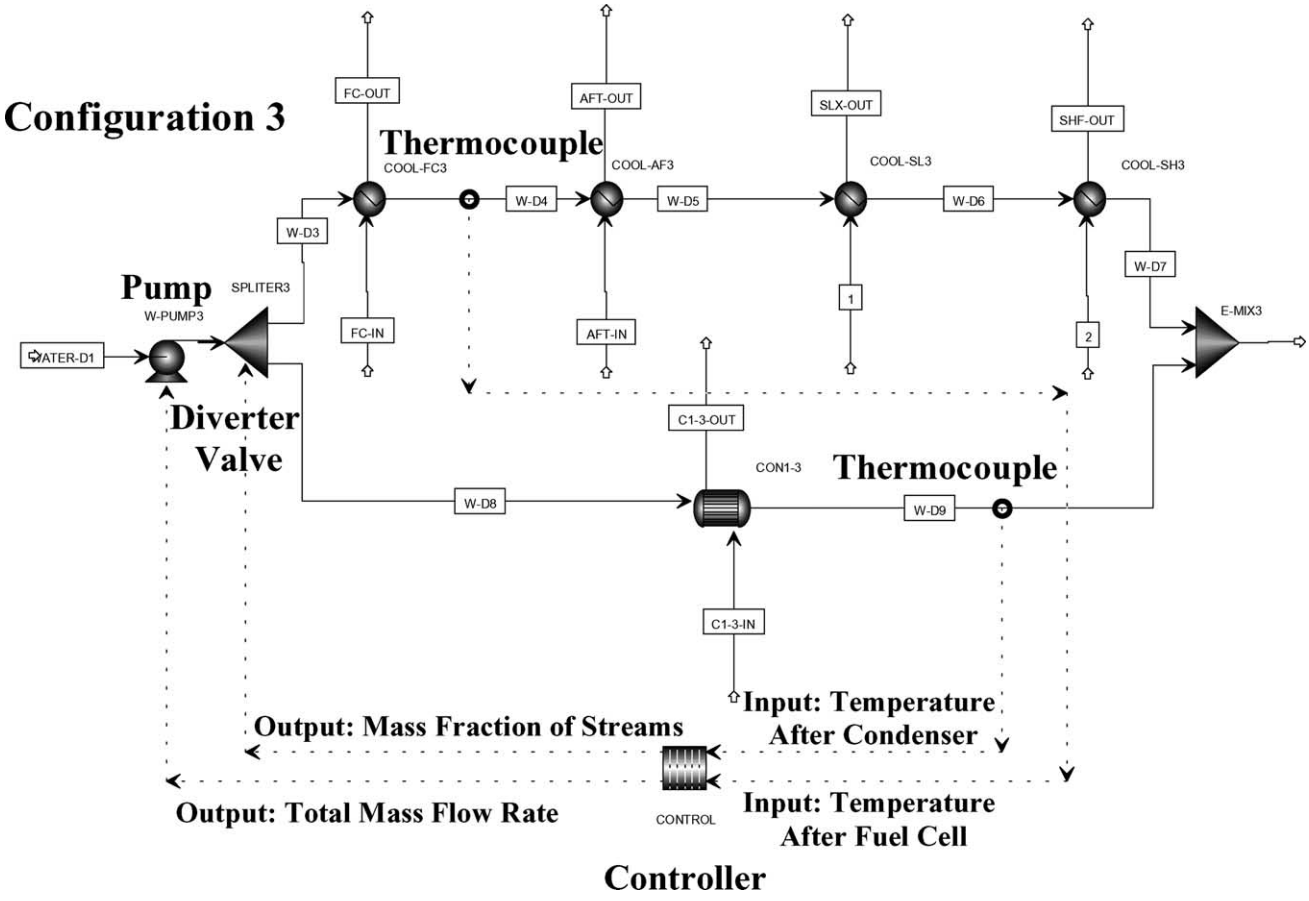

Fig. 17. Cost effective control system for configuration 3.

3.2.4. Configuration 4: Parallel thermal loop with dual condensers

The advantages and disadvantages of Configuration 4 are summarised in Table 6 in the fourth column. Configuration 4 is identical to Configuration 3, with one exception: the condenser is split into separate components, with one condenser at the entrance to the cooling loop. Configuration 4 manages the cooling loop by placing four thermal sources in series with respect to each other and altogether in parallel with respect to part of the fifth thermal source, the high-temperature end of the condenser. The low temperature end of the condenser is placed at the entrance to these loops. This configuration option is only advantageous when the condenser outlet temperature is below the fuel cell coolant outlet temperature. As the condenser outlet temperature is set at 65 °C for the datum design condition (and the fuel cell coolant outlet temperature is set at 60 °C), this configuration is not appropriate for the initial datum design condition given, only at lower condenser outlet temperatures. The primary disadvantages of this configuration are (1) slightly greater system complexity (row two), (2) additional hardware and consequent construction cost (row four), as compared with the primary advantage of (1) higher heat recovery under low condenser temperature outlet conditions (row one).

4. Conclusion

For the 6 kWe combined heat and power (CHP) fuel cell system (FCS) modelled using Aspen Plus® chemical engineering software, the analysis determined the optimal configuration for the system's cooling loop. As shown in Table 6, Configuration 3 (depicted in the schematic diagram of Fig. 9) achieved the highest overall rating for the five key design success factors. This cooling loop configuration achieves (1) a high total thermal energy capture (and liquid water capture), (2) simplicity of design, (3) simplicity of control, (4) low cost construction, and (5) a high system-wide pinch point temperature. This design also achieves a positive system water balance, with no additional water needing to be added to the system. For this optimal cooling configuration, the analysis also assembles useful data for the design of the loop's heat exchangers, as shown in Tables 7 and 8. Such detailed system design studies produce useful recommendations that in turn can help to define a system's control strategy. These complex control strategies allow systems to operate in a more environmentally benign and financially profitable manner.

For combined heat and power (CHP) fuel cell systems (FCS) to achieve a genuine financial and environmental improvement over competing technologies, they must not

only produce electricity at high efficiency, but also efficiently supply heat. As Great Britian's sole commercially-installed CHP FCS shows, in providing heating, cooling, and electricity to Woking's Leisure Centre, these systems must be valued not only for their contribution to electrical power generation, but also for their thermal contribution. Based on an analysis of the potential use of CHP FCSs within energy markets, these systems would appear more economically and environmentally attractive in these markets if three of their inherent technical qualities were further developed. These include (1) their ability to deliver waste heat to a useful thermal sink, (2) their ability to vary their heat to power ratio during operation, and (3) their ability to vary their electrical load rapidly. If developed, these technical qualities could render CHP FCSs a financial and environmental advantage over conventional generation technologies. However, to this, the fuel cell research and development community would have to significantly alter its research trajectory, which has hitherto focused almost myopically on maximising the fuel cell stack's electrical efficiency (voltage).

Acknowledgements

The author wishes to thank the following organisations: The British Marshall Fellowship Committee, http://www.marshallscholarship.org/; The United States (US) National Science Foundation (NSF), http://www.nsf.gov/; The United Kingdom (UK) Department of Trade and Industry (DTI), http://www.dti.gov.uk/; and The Johnson Matthey Technology Centre (JMTC), http://www.matthey.com.

References

[1] W.G. Colella, Combined Heat and Power Fuel Cell Systems, Doctoral Thesis, Department of Engineering Sciences, The University of Oxford, Oxford, 2002.
[2] A.J. Wright, J.R. Formby, Overcoming Barriers to Scheduling Embedded Generation to Support Distribution Networks, Department of Trade and Industry (DTI), London, UK, 2000.
[3] New York State Energy Research and Development Authority (NYSDERA), Evaluation of Packaged Co-generation for Multifamily Residential Applications, Report 91–14, NYSDERA, NY, 1991.
[4] C. Seymour, Commercial Acceptability of Solid Polymer Fuel Cell Systems in the Role of Combined Heat and Power Packages, Department of Trade and Industry (DTI), London, UK, 1998.
[5] D. Hart, A. Bauen, Further Assessment of the Environmental Characteristics of Fuel Cells and Competing Technologies, Department of Trade and Industry (DTI), London, UK, 1998, p. 52.
[6] W.J. Baumol, A.S. Blinder, Economics: Principles and Policy, South-Western Publishers, London, UK, 2000.
[7] W.G. Colella, Design options for achieving a rapidly variable heat-to-power ratio in a combined heat and power (CHP) fuel cell system, J. Power Sources 106 (2002) 388–396.
[8] Data Source: Data from January to December 1998, Office of Electricity and Gas Markets (OFGEM), London, UK, 1998.
[9] Data Source: Data from Five English Houses, EA Technology, Chester, UK, January 2001.
[10] A.C. Stockman, Microeconomics, The Dryden Press Harcourt Brace College Publishers, Fort Worth, TX, 1996, p. 111.
[11] "Enron Rigged Power Market in California, Documents Say", The Wall Street J. May (2002).
[12] C. Parks, "Ex-trader to Plead Guilty in California Scam", Financial Times, 17 October 2002.
[13] D. Newbery, The Regulator's View of the English Electricity Pool, Department of Applied Economics, Cambridge University, Cambridge, UK, 1998.
[14] W.J. Baumol, A.S. Blinder, Economics: Principles and Policy, South-Western Publishers, London, UK, 2000.
[15] A.C. Stockman, Microeconomics, The Dryden Press Harcourt Brace College Publishers, Fort Worth, TX, 1996, p. 356.
[16] "Verluste beim Stromtransport 1999: Strombersorger reduzierten Netzverluste", Press Release, VDEW, The Association of German Utilities, 19 June 2000, http://www.strom.de.
[17] Dresdner Kleinwort Benson, "Appendix A: Electricity Price Setting in a Competitive Market", The New German Electricity Market, Germany, November 1996.
[18] W.G. Colella, Combined Heat and Power Fuel Cell Systems, Transfer Report, Department of Engineering Sciences, The University of Oxford, June 2001.
[19] D. Bauknecht, Market Analyst for the Electricity Industry in Germany, Switzerland, and Austria, Power Ink Plc., Brighton, UK, http://www.power-ink.com.
[20] Dresdner Kleinwort Benson, "Appendix A: Electricity Price Setting in a Competitive Market", The New German Electricity Market, Germany, November 1996.
[21] A.C. Stockman, Microeconomics, The Dryden Press Harcourt Brace College Publishers, Fort Worth, TX, 1996, p. 563.
[22] R. Coase, The problem of social cost, J. Law Econ. October (1960).
[23] D. Bauknecht, W.G. Colella, "Der neue englische Strommarkt NETA und die Folgen für Erneuerbare Energien und KWK-Anlagen", Energiewirtschaftliche Tagesfragen ["The new English electricity market NETA and its consequences for renewables and CHP", Energy Industry (current issues)], June 2002.
[24] W.G. Colella, Implications of electricity liberalization for combined heat and power (CHP) fuel cell systems (FCSs): a case study of the United Kingdom, J. Power Sources 106 (1) (2002) 397.
[25] K. Washington, "Development of a 250 kW class polymer electrolyte fuel cell stack at Ballard Power Systems Inc.", in: Proceedings of the 2000 Fuel Cell Seminar Abstracts: Fuel Cells—Powering the 21st Century, DOE, Portland, OR, US, 2000, p. 468.
[26] P.S. Goulding, A. Gough, M. Deegan, Compact Reformer for the Solid Polymer Fuel Cell, Department of Trade and Industry (DTI), London, UK, 1998.
[27] B. Linnhoff, P. Senior, Energy targets clarify scope for better heat integration, Process Eng. March (1983) 29–33;
B. Linnhoff, J. Turner, Heat recovery networks: new insights yield big savings, Chemical Eng. November (1981) 56–70.
[28] C.B. Snowdon, "Pinch technology: heat exchanger networks", Process Design and Economics C5A, Department of Engineering Sciences, Oxford University Press, Oxford, 2002, p. 21.
[29] D.E. Winterbone, "Pinch technology", Advanced Thermodynamics for Engineers, Butterworths–Heinemann, NY, 1996, p. 47.
[30] Net water diffusion derived from: Buche, Silvain, Polymer Electrolyte Fuel Cell Diagnostics, Doctorate of Philosophy, University of Bath, Bath, UK, 1999, p. 193.
[31] D.R. Lide, "Steam tables", Handbook of Chemistry and Physics, 77th ed. CRC Press, Boca Raton, FL, 1996, pp. 6–17.
[32] W.M. Rohsenow, J.P. Hartnett, Y.I. Cho, Handbook of Heat Transfer, third ed., McGraw-Hill, NY, 1998, p. 17.28.
[33] J.P. Holman, Heat Transfer, seventh ed., McGraw-Hill, NY, 1990, p. 552.